
# Rechargeable zinc-air battery with bifunctional electrocatalyst of copper oxide and graphene nanoplatelets

Electrochemistry Communications 165 (2024) 107760

Contents lists available at ScienceDirect

Electrochemistry Communications

journal homepage: www.elsevier.com/locate/elecom

# Rechargeable zinc-air battery with bifunctional electrocatalyst of copper oxide and graphene nanoplatelets

Barbara A.C. Sá [a], Tatiana S. Andrade [b,*], Rafael R. de Souza [a], Antero R. Santos Neto [a], Mariandry Rodriguez [a], Francisco G.E. Nogueira [c], Márcio C. Pereira [a]

[a] Institute of Science, Engineering, and Technology (ICET), Federal University of Jequitinhonha and Mucuri Valleys (UFVJM), Campus Mucuri, Teófilo Otoni 39803-371, Minas Gerais, Brazil
[b] Department of Electrical Engineering, Chalmers University of Technology, 41258 Gothenburg, Sweden
[c] Department of Chemical Engineering, Federal University of São Carlos (UFSCar), São Carlos 13565-905, São Paulo, Brazil

ARTICLE INFO

*Keywords:*
Metal-air batteries
Zn-air batteries
Secondary zinc-air batteries
ORR
OER
Bifunctional oxygen electrocatalysts

ABSTRACT

Rechargeable zinc-air batteries have been identified as promising technologies for energy storage. However, developing cost-effective electrocatalysts that can efficiently facilitate the oxygen evolution reaction (OER) and oxygen reduction reaction (ORR) is crucial for their advancement. This work investigates synthesized electrocatalysts composed of graphene-$Cu_2O$ deposited on carbon cloth by doctor blading casting method as bifunctional electrodes in a rechargeable Zn-air battery. The battery integrated with graphene-$Cu_2O$ as the air-cathode electrocatalyst showed superior performance in terms of cycling stability compared to that without $Cu_2O$. This enhanced performance is attributed to the reversibility of $Cu^{+}/Cu^{2+}$ species during the redox reactions facilitated by the high electrical conductivity of graphene. Therefore, the results suggest the potential of the synthesized electrodes for advancing the development of rechargeable Zn-air batteries.

## 1. Introduction

Zinc-air batteries (ZABs) have emerged as promising alternative energy storage technologies due to their safer design, lower cost, and higher theoretical energy density than the current commercialized lithium-ion batteries [1–4]. ZABs consist of zinc and air electrodes separated by an electrolyte, usually an aqueous alkaline solution. These batteries generate electricity through zinc oxidation in the metal electrode, whereas the oxygen reduction reaction (ORR) occurs in the air-electrocatalyst. For rechargeable ZABs (RZABs), opposite reactions occur during charging: the zinc reduction in the metal electrode and the oxygen evolution reaction (OER) in the air electrode. However, RZABs still face issues regarding their cyclability performance, making developing novel electrocatalysts crucial for enhancing their power density, specific capacity, and round efficiency [5–8]. Noble metal-based catalysts such as platinum (Pt) and ruthenium and iridium oxides ($RuO_2$ and $IrO_2$) have shown desirable electrocatalytic activities, but their high costs limit the large-scale commercial applications of rechargeable zinc-air batteries. Therefore, efforts have been directed toward investigating electrocatalysts based on earth-abundant elements that aim to achieve high electrocatalytic performance and competitive cost [9–11].

Combining carbon materials with metal oxides is a promising approach for creating cost-efficient materials with enhanced electrocatalytic performances. Carbon-based materials, such as graphene and carbon-black, can increase conductivity and surface area, while metal oxides can improve catalytic activity and potentially reduce costs due to their abundance on Earth. However, finding metal-oxides that can act as bifunctional electrocatalysts for the oxygen reduction reaction (ORR) and oxygen evolution reaction (OER) in RZABs remains challenging. Most studies on metal-oxides as bifunctional air electrodes for RZABs have focused on $CoO_x$, $MnO_x$, and $FeO_x$ [12–20]. These metals have incomplete orbitals, allowing electron movement and thus the ORR and OER catalysis. For instance, $Co_3O_4$ is one of the most investigated metal-oxides for ZABs and promotes the OER through its $Co^{2+}$ species, while the $Co^{3+}$ species can support the ORR [21]. In this regard, $CuO_x$ also appears to be a promising alternative for bifunctional air-electrocatalysts because of its incomplete d-orbital, which allows for easy interconversion between $Cu^{+}$ and $Cu^{2+}$ species. $CuO_x$ has been widely applied in photoelectrochemistry, including photo-electrocatalytic fuel cells and photoelectrocatalytic batteries [22–26].

* Corresponding author.
*E-mail address:* tatianas@chalmers.se (T.S. Andrade).

https://doi.org/10.1016/j.elecom.2024.107760
Received 20 February 2024; Received in revised form 17 May 2024; Accepted 19 May 2024
Available online 20 May 2024

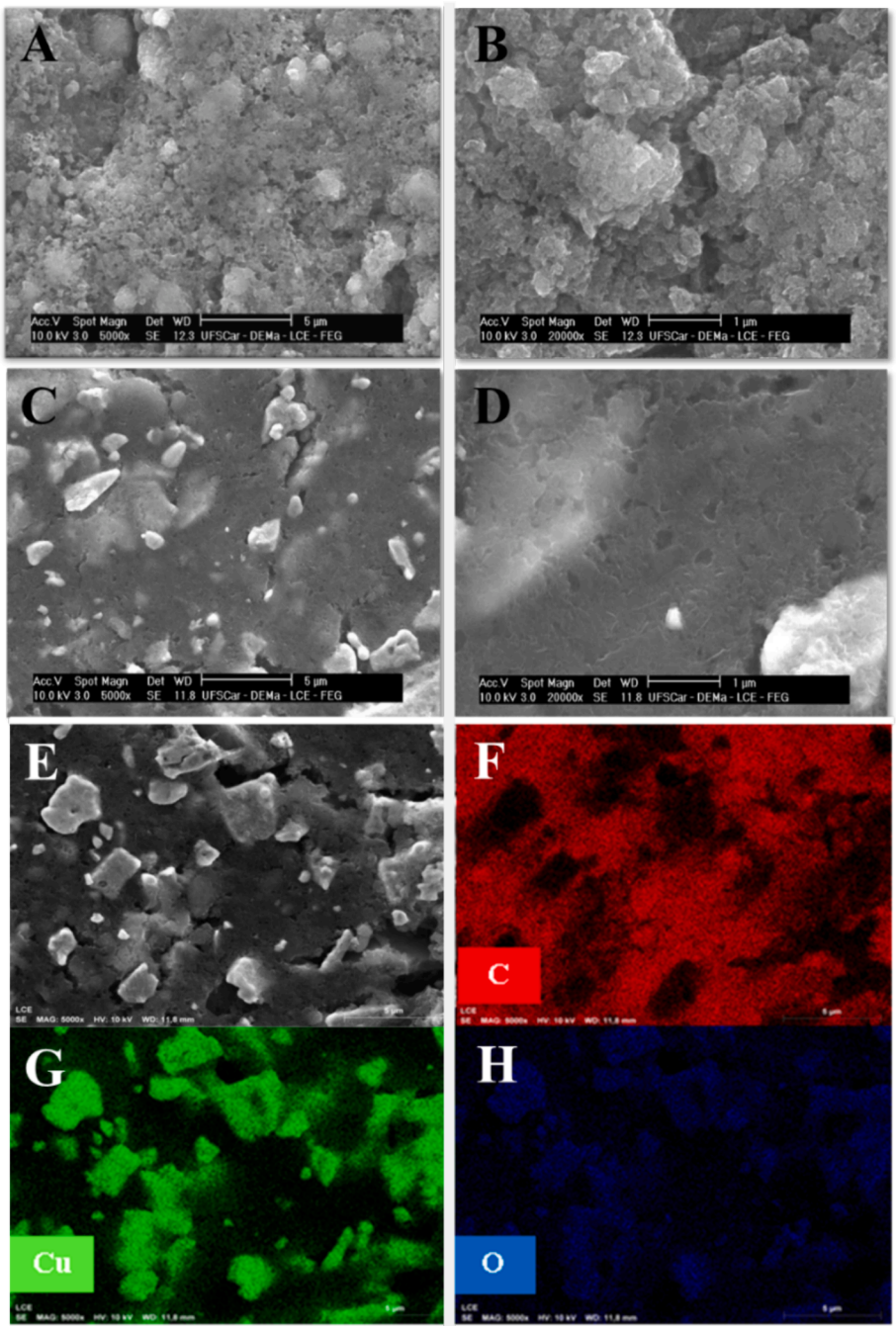


**Fig. 1.** SEM images of graphene (A, B) and graphene with $Cu_2O$ (C, D) films, and EDS mappings of elements C, Cu, and O for the graphene-$Cu_2O$ film.

However, copper oxides combined with graphene have not yet been reported as a bifunctional air-electrode for RZABs. Thus, this study aims to investigate the potential use of $Cu_2O$ coupled with graphene nanoplatelets as a bifunctional electrocatalyst for OER and ORR in rechargeable Zn-air batteries.

## 2. Materials and methods

### 2.1. Electrode synthesis

All materials used were analytical grade and sourced from Sigma Aldrich unless otherwise specified. Carbon cloth (CC) was obtained from Fuel Cell Earth (Wobum, MA, USA). The synthesized electrode was composed of a graphene-based paste, which was deposited on carbon cloth as the electrocatalyst. The graphene-based paste was prepared as reported previously [27]. 1 g of graphene was mixed with 5 mL of distilled water and 0.4 mL polytetrafluorethylene (Teflon 60 % wt. dispersion in water) by vigorous mixing to create a viscous paste. For the paste containing copper oxides, 4 g of $Cu_2O$ was also added. The quantity of $Cu_2O$ used was determined through pre-experiments, which showed slightly better short-circuit current values with this amount, but further increasing it resulted in the paste becoming too viscous to deposit. It was also found that without graphene, the film was not hydrophobic and could not be deposited on the carbon cloth surface. The paste was deposited on the carbon cloth by doctor blade casting using a spatula, and the electrode was annealed in an oven at 340 °C for 15 min in the ambient atmosphere. This procedure was repeated once to ensure that the carbon cloth was completely covered with the carbon layer, resulting in approximately 0.03 g $cm^{-2}$ of dried paste for each electrode.

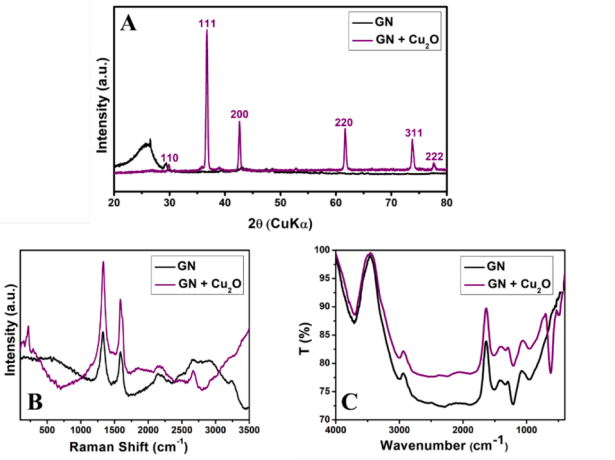


**Fig. 2.** XRD pattern (A), Raman (B), and FTIR (C) spectra of the samples GN and GN-$Cu_2O$.

### 2.2. Structural and morphological characterization

The structural and morphological properties of the electrodes synthesized with and without $Cu_2O$ were investigated by scanning electron microscope (SEM), energy dispersive spectroscopy (EDS), X-ray diffraction (XRD), Raman, and infrared spectroscopy. The SEM and EDS examinations were carried out using a tungsten electron source operating at a potential of 10 kV. For SEM, the secondary electron (ES) mode was employed at magnifications of 5000x and 20000x. The XRD measurements were conducted using a 2θ range ranging from 5 to 80°, with a scanning speed of 2° $min^{-1}$, and Cu Kα radiation (λ = 1.54056 Å) at 30 kV and 30 mA on a Rigaku diffractometer Miniflex 600. Raman spectra were obtained using an Olympus TM BX41 microscope coupled with a Horiba Jobin-Yvon Raman LabRAM micro spectrometer at room temperature with a He-Ne laser line as the excitation source.

### 2.3. Electrochemical measurements

The electrochemical characterization was conducted using an active area of 1.0 $cm^2$ on the electrodes in the reactor. The air-electrode side covered with the catalyst was placed in contact with the electrolyte, while the other side was exposed to ambient air, facilitating oxygen entry. Electrochemical characterization was performed using 3 and 2-electrode configurations to assess the performance of the air electrode and the battery performance, respectively. A reference electrode is also used in a 3-electrode characterization, besides the working electrode and the counter electrode. For the 3-electrode configuration, the synthesized electrocatalysts deposited on the carbon cloth were used as the working electrode, while an Ag/AgCl (3 M KCl) electrode served as the reference electrode, and a Pt foil was used as the counter electrode. The electrodes were immersed in a 0.1 M KOH aqueous electrolyte. For the zinc-air battery characterization, the synthesized electrodes (electrocatalysts on the carbon cloth) were used as the air electrode, and a zinc-foil was used as the metal electrode. The measurements were performed

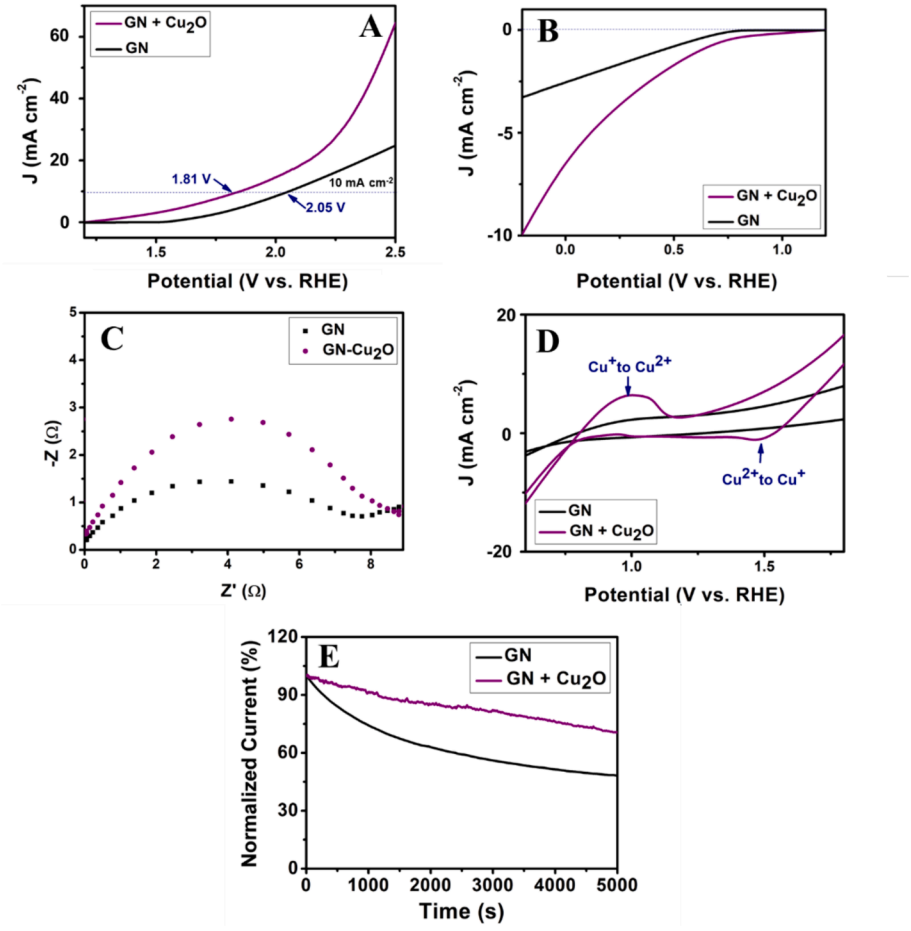


**Fig. 3.** OER (A) and ORR (B) polarization curves, electrochemical impedance spectroscopy (C) cyclic voltammograms (D), and current–time chronoamperometric responses (E) for GN and GN-$Cu_2O$ electrodes in alkaline media (0.1 M KOH).

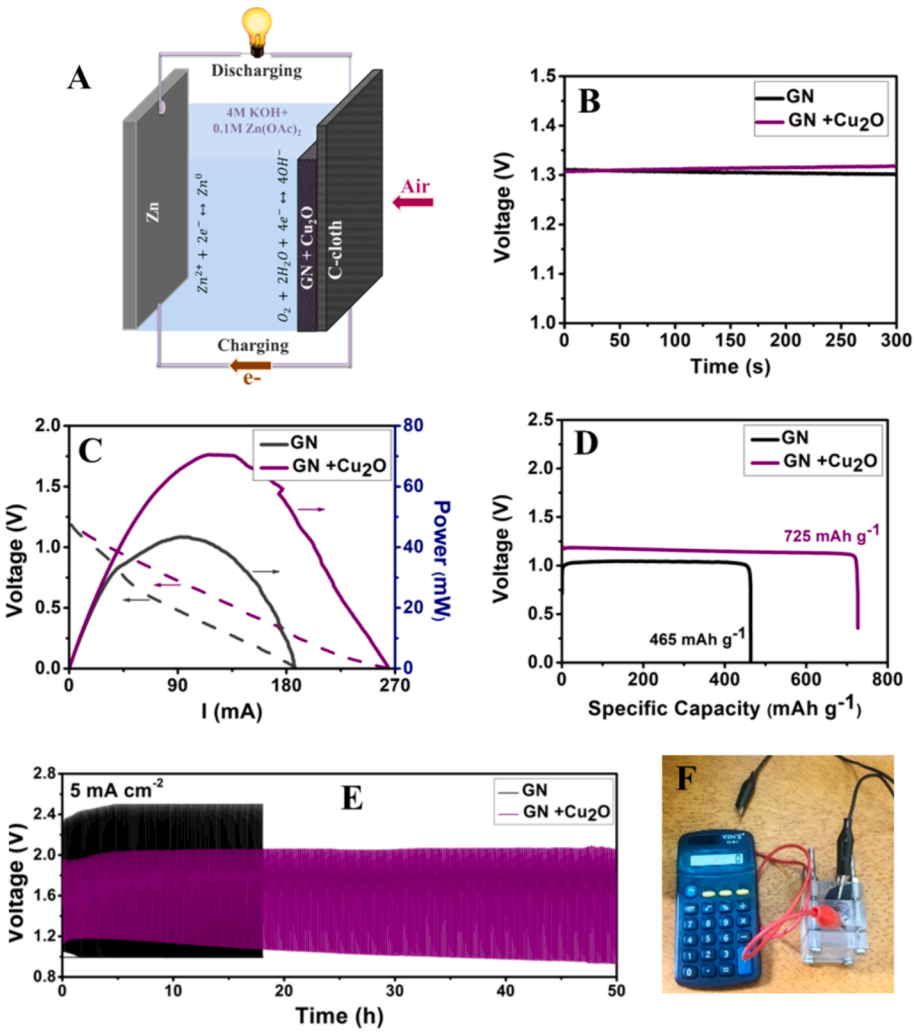


**Fig. 4.** Rechargeable Zn-air battery schematic representation (A). OCV measurements (B), IV, and power curves (C), specific discharging capacities at 10 mA $cm^{-2}$ (D), and charging-discharging cycles of the batteries composed of GN or GN-$Cu_2O$ electrodes at 300-second cycles, i.e. shallow cycling (E). Demonstration of the constructed battery connected to a calculator (F).

in a one-compartment plexiglass reactor filled with 4 M aqueous KOH and 0.1 M $Zn(CH_3COO)_2$.

## 3. Results and discussion

### 3.1. Structural and morphological electrode characterization

SEM images of the graphene electrode without $Cu_2O$ particles revealed a porous, sponge-like structure, as shown in Fig. 1A-B. Conversely, adding $Cu_2O$ particles resulted in a more rigid morphology with nanometric clusters, which clearly indicated the $Cu_2O$ incorporation onto graphene support, as shown in Fig. 1C-D. The EDS mapping images of the GN-$Cu_2O$ film confirmed the distribution of carbon (C) throughout the surface and the filling of gaps by oxygen (O) and copper (Cu) atoms, as seen in Fig. 1F-H.

The X-ray diffraction analysis of the GN-$Cu_2O$ electrode revealed the cubic crystalline phase of $Cu_2O$ (JCPDS #05-0667) identified by its Miller indices of (110), (111), (200), (220), (311), and (222) (Fig. 2A). Conversely, no crystalline phase is detected in the GN electrode. The Raman spectra of the graphene film showed D and G bands at 1333 and 1586 $cm^{-1}$, respectively, with the intensity ratio (ID/IG) of the two bands indicating graphene defect. Adding $Cu_2O$ particles increases the disorder, i.e. ID/IG from 1.06 to 1.11, and the oxygen-containing groups, as seen in Fig. 2B [28–31]. The Raman shift at 635 $cm^{-1}$ can be associated with the presence of $Cu_2O$ in the carbon structure [30,32]. The FTIR spectra (Fig. 2C), revealed a band at 620 $cm^{-1}$ for GN-$Cu_2O$, characteristic of the Cu–O vibration. The other bands in both samples can be attributed to the vibration of C═C bonds in the carbon network at 1578 $cm^{-1}$ and the weak O–H vibration at 3450 $cm^{-1}$ [31,33].

### 3.2. Electrochemical activities

The findings from the electrochemical characterization demonstrated that modifying the air-electrode with GN-$Cu_2O$ electrocatalyst had a positive impact on the oxygen evolution reaction (OER) and oxygen reduction reaction (ORR), suggesting that GN-$Cu_2O$ could be applied as a bifunctional electrocatalyst for RZABs. The linear voltammogram (Fig. 3A) revealed a decrease in the onset potential for the OER, from 2.05 V using the GN electrode to 1.81 V vs. RHE using the GN-$Cu_2O$. Additionally, the ORR activity is poor with $E_{1/2}$ close to zero for the GN electrocatalyst and about 0.25 V vs. RHE for the GN-$Cu_2O$ (Fig. 3B). These results indicate that the GN-$Cu_2O$ electrode can improve battery discharging and charging, making it a promising candidate for bifunctional electrodes. The electrochemical impedance spectroscopy (EIS) revealed similar charger transfer resistance to the electrocatalyst of GN-$Cu_2O$ compared to the GN electrocatalyst ($R_{CT}$-GN-$Cu_2O$ = 8.5 Ω and $R_{CT}$-GN = 8.0 Ω), as shown in Fig. 3C. Nevertheless, the higher catalytic activity of the GN-$Cu_2O$ electrode can be attributed to the reversibility

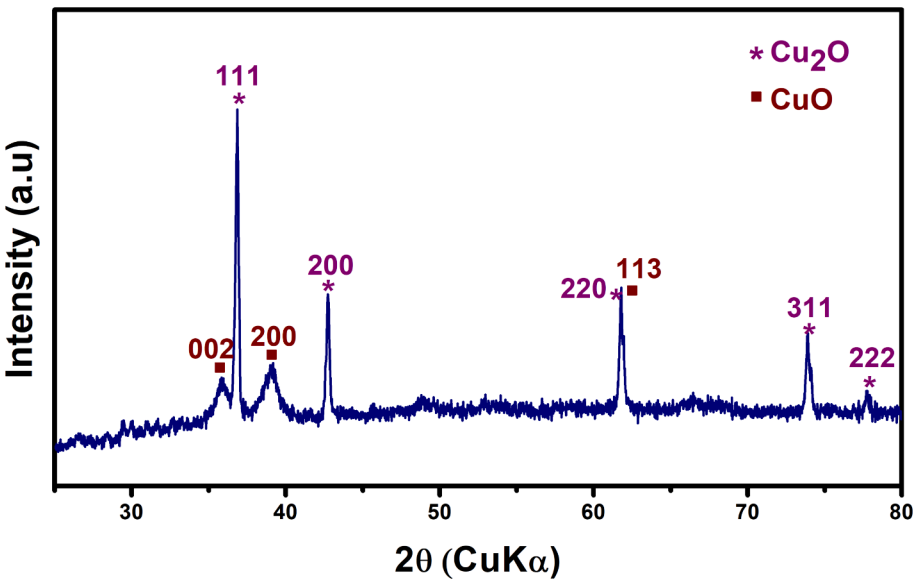


**Fig. 5.** XRD pattern for the electrocatalyst GN-$Cu_2O$ after the battery operation.

between $Cu^{2+}$ and $Cu^{+}$ ions, as identified in the cyclic voltammogram shown in Fig. 3D. This switch in the Cu ions has also been observed in recent investigations of novel electrocatalysts for Zn-air batteries, but only under lighting or coupled with $Co_3O_4$ [22,34]. In this work, the high conductivity of graphene is associated with the promotion of Cu speciation. Therefore, the double oxidation state of Cu ions generated at the OER and ORR potentials should boost the catalysis of redox reactions during battery operation. Furthermore, the stability test of the electrode at a constant potential of −0.6 V vs. Ag/AgCl (Fig. 3D) demonstrated the superior performance of the GN-$Cu_2O$ electrode, with over 70 % of its original current remaining after several hours, confirming its potential for use in rechargeable Zn-air batteries.

### 3.3. Rechargeable zinc-air batteries

To assess the functionality of the rechargeable Zn-air battery electrodes, we implemented and tested the scheme depicted in Fig. 4A using either the GN or the GN-$Cu_2O$ sample as the electrocatalyst deposited on carbon cloth. The results showed similar open-circuit voltages (OCV) of approximately 1.3 V for both batteries (Fig. 4B). This agrees with previous results that show that the practical OCVs of Zn-air batteries are lower than the theoretical 1.6 due to overpotential losses. However, the short-circuit current and power density of the battery with the GN-$Cu_2O$ electrocatalyst were significantly higher than those without $Cu_2O$ in the air-electrode. The values of the short-circuit current and power density ranged from 190 to 260 mA and 42 to 75 mW, respectively, as shown in Fig. 4C. Other studies that use metal oxides, e.g., $Co_3O_4$, $NiCo_2O_4$, with graphene have reported power density in the range of 50–200 mW $cm^{-2}$. The relative increase in power density compared to the reference sample used in those studies was in the range of 50–56 %. Meanwhile, in this work, the relative increase was about 78 %, demonstrating the positive effect of the $Cu_2O$ on the battery performance [35–38]. The battery with the GN-$Cu_2O$ electrocatalyst also had a higher specific capacity of 725 mAh $g^{-1}$ at a continuous current of 10 mA, as compared to 465 mAh $g^{-1}$ for the battery without $Cu_2O$ (Fig. 4D). The relative improvement shown to the specific capacity provided by the $Cu_2O$ was also more significant than other reported metal oxides combined with graphene [35–38]. Further, the charge–discharge stability test demonstrated the potential of the GN-$Cu_2O$ for use as a bifunctional electrocatalyst in RZABs, with a lower voltage change for charge and discharge potentials, consistently with experimental findings shown in Fig. 3A-B, as well as a superior cyclability The battery with the GN-$Cu_2O$ electrode remained stable for 50 h, as shown in Fig. 4E. Finally, the practical applicability of the battery is demonstrated by connecting it to a calculator, as shown in Fig. 4F. After the battery application, the XRD pattern for the electrocatalyst has revealed both $Cu_2O$ and CuO phases, as shown in Fig. 5, supporting the existence of the redox couple $Cu^{+}$ and $Cu^{2+}$ during the operation. Table 1 presents the performance of reported ZABs that used electrocatalysts composed of graphene/carbon-based materials, or/and $Cu_2O$ or other metal oxides.

**Table 1**

| Electrocatalyst | Peak power density ( *) | Specific capacity ( *) | Reference |
|---|---|---|---|
| Graphene-$Cu_2O$ | 75 mW $cm^{-2}$ (78 %) | 725 mAh $g^{-1}$ (56 %) | This work |
| ZnO/$Cu_2O$ | 8 mW $cm^{-2}$ (85 %) | 334 mAh $g^{-1}$ (–) | [22] |
| Ccube/$Cu_2O$/$Co_3O_4$ | 219 mW $cm^{-2}$ (15 %) | 781 mAh $g^{-1}$ (–) | [34] |
| rGO/$NiCo_2O_4$ | 125 mW $cm^{-2}$ (26 %) | 720 mAh $g^{-1}$ (–) | [35] |
| rGO-Co@$Co_3O_4$/FeNS | 181 mW $cm^{-2}$ (51 %) | – | [36] |
| N-rGO/$Co_3O_4$ | 47 mW $cm^{-2}$ (56 %) | 875 mAh $g^{-1}$ (15 %) | [37] |
| N-graphene/CoO | 135 mW $cm^{-2}$ (48 %) | 815 mAh $g^{-1}$ (4 %) | [38] |
| Cnanotube-$Co_3O_4$ | 267 mW $cm^{-2}$ (5 %) | 814 mAh $g^{-1}$ (3 %) | [39] |
| Cspheres/$Mn_3O_4$ | 183 mW $cm^{-2}$ (16 %) | – | [40] |
| Cnanotube/ $Mn_3O_4$ | 87 mW $cm^{-2}$ (18 %) | 823 mAh $g^{-1}$ (–) | [41] |
| $MnO_x$/CC | 148 mW $cm^{-2}$ (17 %) | 816 mAh $g^{-1}$ (–) | [42] |
| $Fe_3O_4$/N-C nanoflower | 137 mW $cm^{-2}$ (42 %) | 749 mAh $g^{-1}$ (11 %) | [43] |
| $Fe_3O_4$/N-carbon spheres | 141 mW $cm^{-2}$ (64 %) | 723 mAh $g^{-1}$ (11 %) | [44] |

* Increase relative to reference sample.

## 4. Conclusion

In this work, we investigated the potential of a bifunctional electrode composed of $Cu_2O$ and graphene for use in a rechargeable zinc-air battery. Electrochemical characterization showed that the electrode could carry out both the OER and ORR due to the reversibility of $Cu^{+}$/$Cu^{2+}$ ions within the redox voltage range. When applied to the

rechargeable Zn-air battery, the device demonstrated higher power, specific capacity, and stability than batteries without the $Cu_2O$ component. Therefore, this study highlights the potential of graphene-$Cu_2O$ electrocatalysts for use in rechargeable Zn-air batteries, which could contribute to the advancement of such technologies.

## CRediT authorship contribution statement

**Barbara A.C. Sá:** Writing – review & editing, Methodology, Investigation. **Tatiana S. Andrade:** Writing – original draft, Supervision, Conceptualization. **Rafael R. de Souza:** Writing – review & editing, Investigation. **Antero R. Santos Neto:** Writing – review & editing. **Mariandry Rodriguez:** Writing – review & editing. **Francisco G.E. Nogueira:** Writing – review & editing, Resources. **Márcio C. Pereira:** Writing – review & editing, Supervision, Project administration, Funding acquisition.

## Declaration of competing interest

The authors declare that they have no known competing financial interests or personal relationships that could have appeared to influence the work reported in this paper.

## Data availability

Data will be made available on request.

## Acknowledgments

The authors thank FAPEMIG (grant numbers REDE-113/10; RED00520-16; CEX-112-10; CEX-RED-00010–14; PPM-00104-17), CNPq (grant numbers 442820/2014-3; 304598/2014-3; 301839/2017-4; INCT MIDAS), FAPESP (2018/09723-9), FINEP/MCTI, and CAPES (Code 001) for the financial support. T.S.A. thanks Chalmers' Area of Advance Transport for the postdoctoral fellowship.

## References

[1] Y. Li, H. Dai, Recent advances in Zinc-air batteries, Chem. Soc. Rev. 43 (2014) 5257–5275, https://doi.org/10.1039/c4cs00015c.
[2] J. Zhang, Q. Zhou, Y. Tang, L. Zhang, Y. Li, Zinc-air batteries: Are they ready for prime time? Chem. Sci. 10 (2019) 8924–8929, https://doi.org/10.1039/c9sc04221k.
[3] N. Shang, K. Wang, M. Wei, Y. Zuo, P. Zhang, H. Wang, Z. Chen, P. Pei, Challenges for large scale applications of rechargeable Zn-air batteries, J. Mater. Chem. A 10 (2022) 16369–16389, https://doi.org/10.1039/d2ta04294k.
[4] D. Yang, H. Tan, X. Rui, Y. Yu, Electrode materials for rechargeable zinc-ion and zinc-air batteries: current status and future, Perspectives (2019), https://doi.org/10.1007/s41918-019-00035-5.
[5] X. Chen, Z. Zhou, H.E. Karahan, Q. Shao, L. Wei, Y. Chen, Recent advances in materials and design of electrochemically rechargeable zinc-air batteries, Small. 14 (2018) 1–29, https://doi.org/10.1002/smll.201801929.
[6] M. Luo, W. Sun, B. Bin Xu, H. Pan, Y. Jiang, Interface engineering of air electrocatalysts for rechargeable zinc-air batteries, Adv. Energy Mater. 11 (2021) 1–14, https://doi.org/10.1002/aenm.202002762.
[7] J. Fu, Z.P. Cano, M.G. Park, A. Yu, M. Fowler, Z. Chen, Electrically rechargeable zinc-air batteries: progress, challenges, and perspectives, Adv. Mater. 29 (2017), https://doi.org/10.1002/adma.201604685.
[8] Q. Wang, S. Kaushik, X. Xiao, Q. Xu, Sustainable zinc-air battery chemistry: advances, challenges and prospects, Chem. Soc. Rev. 52 (2023) 6139–6190, https://doi.org/10.1039/d2cs00684g.
[9] Y.-F. Guo, Y. Li, Y.-H. Chen, P.-F. Wang, Y. Xie, T.-F. Yi, Rational design of one-dimensional cobalt-related oxygen electrocatalysts toward high-performance zinc-air batteries, Coord. Chem. Rev. 495 (2023) 215383.
[10] L. Peng, L. Shang, T. Zhang, G.I.N. Waterhouse, Recent advances in the development of single-atom catalysts for oxygen electrocatalysis and zinc-air batteries, Adv. Energy Mater. 10 (2020) 1–22, https://doi.org/10.1002/aenm.202003018.
[11] A. Kundu, S. Mallick, S. Ghora, C.R. Raj, Advanced oxygen electrocatalyst for air-breathing electrode in Zn-air batteries, ACS Appl. Mater. Interfaces. 13 (2021) 40172–40199.
[12] Z. Yang, H. Yuan, C. Zhou, Y. Wu, W. Tang, S. Sang, H. Liu, Facile interfacial adhesion enabled LATP-based solid-state lithium metal battery, Chem. Eng. J. 392 (2020) 123650, https://doi.org/10.1016/J.CEJ.2019.123650.
[13] Y. Zhao, X. Zhou, L. Ye, S. Chi Edman Tsang, Nanostructured $Nb_2O_5$ catalysts, Nano Rev. 3 (2012) 17631, https://doi.org/10.3402/nano.v3i0.17631.
[14] R. Marschall, Semiconductor composites: strategies for enhancing charge carrier separation to improve photocatalytic activity, Adv. Funct. Mater. 24 (2014) 2421–2440, https://doi.org/10.1002/adfm.201303214.
[15] K. Trzciński, M. Szkoda, M. Sawczak, A. Lisowska-Oleksiak, Enhanced photoelectrocatalytical performance of inorganic-inorganic hybrid consisting $BiVO_4$, V2O5, and cobalt hexacyanocobaltate as a perspective photoanode for water splitting, Electrocatalysis 11 (2020) 180–187, https://doi.org/10.1007/S12678-019-00566-X.
[16] D. Du, S. Zhao, Z. Zhu, F. Li, J. Chen, Photo-excited oxygen reduction and oxygen evolution reactions enable a high-performance Zn–air battery, Angew. Chemie - Int. Ed. 59 (2020) 18140–18144, https://doi.org/10.1002/anie.202005929.
[17] P. Gu, M. Zheng, Q. Zhao, X. Xiao, H. Xue, H. Pang, Rechargeable zinc-air batteries: a promising way to green energy, J. Mater. Chem. A 5 (2017) 7651–7666, https://doi.org/10.1039/c7ta01693j.
[18] Y. Tian, L. Xu, J. Qian, J. Bao, C. Yan, H. Li, H. Li, S. Zhang, $Fe_3C/Fe_2O_3$ heterostructure embedded in N-doped graphene as a bifunctional catalyst for quasi-solid-state zinc–air batteries, Carbon N. Y. 146 (2019) 763–771, https://doi.org/10.1016/j.carbon.2019.02.046.
[19] M. Mechili, C. Vaitsis, N. Argirusis, P.K. Pandis, G. Sourkouni, C. Argirusis, Research progress in transition metal oxide based bifunctional electrocatalysts for aqueous electrically rechargeable zinc-air batteries, Renew. Sustain. Energy Rev. 156 (2022), https://doi.org/10.1016/j.rser.2021.111970.
[20] D.U. Lee, J. Scott, H.W. Park, S. Abureden, J.Y. Choi, Z. Chen, Morphologically controlled $Co_3O_4$ nanodisks as practical bi-functional catalyst for rechargeable zinc-air battery applications, Electrochem. Commun. 43 (2014) 109–112, https://doi.org/10.1016/j.elecom.2014.03.020.
[21] Y. Dai, J. Yu, M. Ni, Z. Shao, Rational design of spinel oxides as bifunctional oxygen electrocatalysts for rechargeable Zn-air batteries, Chem. Phys. Rev. 1 (2020) 11303, https://doi.org/10.1063/5.0017398.
[22] D. Bu, M. Batmunkh, Y. Zhang, Y. Li, B. Qian, Y. Lan, X. Hou, S. Li, B. Jia, X. M. Song, T. Ma, Rechargeable sunlight-promoted Zn-air battery constructed by bifunctional oxygen photoelectrodes: energy-band switching between ZnO/$Cu_2O$ and ZnO/CuO in charge-discharge cycles, Chem. Eng. J. 433 (2022), https://doi.org/10.1016/j.cej.2021.133559.
[23] X.X. Ma, L. Chen, Z. Zhang, J.L. Tang, Electrochemical performance evaluation of CuO@$Cu_2O$ nanowires array on Cu foam as bifunctional electrocatalyst for efficient water splitting, Chinese J. Anal. Chem. 48 (2020) e20001–e20012, https://doi.org/10.1016/S1872-2040(19)61211-9.
[24] T.S. Andrade, B.A.C. Sá, F.G.E. Nogueira, L.C.A. Oliveira, M.C. Pereira, Unassisted photocatalytic hydrogen peroxide fuel cell based on dual photoelectrodes with high performance and stability, J. Appl. Electrochem. 53 (2023) 435–444, https://doi.org/10.1007/s10800-022-01790-y.
[25] S. Selvanathan, P. Meng Woi, V. Selvanathan, M.R. Karim, K. Sopian, M. Akhtaruzzaman, Transition metals-based water splitting electrocatalysts on copper-based substrates: the integral role of morphological properties, Chem. Rec. (2023) 202300228, https://doi.org/10.1002/tcr.202300228.
[26] T.S. Andrade, B.A.C. Sá, I.C. Sena, A.R.S. Neto, F.G.E. Nogueira, P. Lianos, M. C. Pereira, A photoassisted hydrogen peroxide fuel cell using dual photoelectrodes under tandem illumination for electricity generation, J. Electroanal. Chem. 881 (2021) 114948, https://doi.org/10.1016/j.jelechem.2020.114948.
[27] P. Katsoufis, M. Katsaiti, C. Mourelas, T.S. Andrade, V. Dracopoulos, C. Politis, G. Avgouropoulos, P. Lianos, Study of a thin film aluminum-air battery, Energies 13 (2020) 1–9, https://doi.org/10.3390/en13061447.
[28] A.R. Thiruppathi, B. Sidhureddy, W. Keeler, A. Chen, Facile one-pot synthesis of fluorinated graphene oxide for electrochemical sensing of heavy metal ions, Electrochem. Commun. 76 (2017) 42–46, https://doi.org/10.1016/j.elecom.2017.01.015.
[29] J.A.V. Piñas, T.S. Andrade, A.T. Oliveira, P.E.A. Salomão, M. Rodriguez, A.C. Silva, H.S. Oliveira, D.S. Monteiro, M.C. Pereira, Production of reduced graphene oxide platelets from graphite flakes using the Fenton reaction as an alternative to harmful oxidizing agents, J. Nanomater. 2019 (2019), https://doi.org/10.1155/2019/5736563.
[30] J. Gu, L. Li, D. Huang, L. Jiang, L. Liu, F. Li, A. Pang, X. Guo, B. Tao, In Situ synthesis of graphene@cuprous oxide nanocomposite incorporated marine antifouling coating with elevated antifouling performance, Open J. Org. Polym. Mater. 09 (2019) 47–62, https://doi.org/10.4236/ojopm.2019.93003.
[31] C. Nethravathi, M. Rajamathi, Chemically modified graphene sheets produced by the solvothermal reduction of colloidal dispersions of graphite oxide, Carbon N. Y. 46 (2008) 1994–1998, https://doi.org/10.1016/j.carbon.2008.08.013.
[32] K. Reimann, K. Syassen, Raman scattering and photoluminescence in $Cu_2O$ under hydrostatic pressure, Phys. Rev. B 39 (1989) 11113–11119, https://doi.org/10.1103/PhysRevB.39.11113.
[33] Y.C. Zhang, J.Y. Tang, G.L. Wang, M. Zhang, X.Y. Hu, Facile synthesis of submicron $Cu_2O$ and CuO crystallites from a solid metallorganic molecular precursor, J. Cryst. Growth 294 (2006) 278–282, https://doi.org/10.1016/j.jcrysgro.2006.06.038.
[34] J. Liu, J. Xie, R. Wang, B. Liu, X. Meng, X. Xu, B. Tang, Z. Cai, J. Zou, Interfacial electron modulation of $Cu_2O$ by $Co_3O_4$ embedded in hollow carbon cube skeleton for boosting oxygen reduction/revolution reactions, Chem. Eng. J. 450 (2022), https://doi.org/10.1016/j.cej.2022.137961.
[35] Y. Li, G. Cheng, Z. Zhou, X. Liao, S. Han, F. Ye, M. Sun, L. Yu, Shape-controlled synthesis of $NiCo_2O_4$-rGO as bifunctional electrocatalyst for Zn-air battery, ChemElectroChem. 6 (2019) 4429–4436.
[36] J. Zhu, W. Tu, Z. Bai, H. Pan, P. Ji, H. Zhang, Z. Deng, H. Zhang, Zeolitic-imidazolate-framework-derived Co@ $Co_3O_4$ embedded into iron, nitrogen, sulfur

Co-doped reduced graphene oxide as efficient electrocatalysts for overall water splitting and zinc-air batteries, Electrochim. Acta 323 (2019) 134821.
[37] J.S. Sanchez, R.R. Maça, A. Pendashteh, V. Etacheri, M. Castillo-Rodríguez, J. Palma, R. Marcilla, Hierarchical $Co_3O_4$ nanorods anchored on nitrogen doped reduced graphene oxide: a highly efficient bifunctional electrocatalyst for rechargeable Zn–air batteries, Catal. Sci. Technol. 10 (2020) 1444–1457.
[38] L. Xu, C. Wang, D. Deng, Y. Tian, X. He, G. Lu, J. Qian, S. Yuan, H. Li, Cobalt oxide nanoparticles/nitrogen-doped graphene as the highly efficient oxygen reduction electrocatalyst for rechargeable zinc-air batteries, ACS Sustain. Chem. Eng. 8 (2019) 343–350.
[39] C.C. Wang, K.Y. Hung, T.E. Ko, S. Hosseini, Y.Y. Li, Carbon-nanotube-grafted and nano- $Co_3O_4$-doped porous carbon derived from metal-organic framework as an excellent bifunctional catalyst for zinc–air battery, J. Power Sources. 452 (2020), https://doi.org/10.1016/j.jpowsour.2020.227841.
[40] Y. He, D. Aasen, H. Yu, M. Labbe, D.G. Ivey, J.G.C. Veinot, $Mn_3O_4$ nanoparticle-decorated hollow mesoporous carbon spheres as an efficient catalyst for oxygen reduction reaction in Zn-air batteries, Nanoscale Adv. 2 (2020) 3367–3374, https://doi.org/10.1039/d0na00428f.
[41] L. Li, J. Yang, H. Yang, L. Zhang, J. Shao, W. Huang, B. Liu, X. Dong, Anchoring $Mn_3O_4$ nanoparticles on oxygen functionalized carbon nanotubes as bifunctional catalyst for rechargeable zinc-air battery, ACS Appl. Energy Mater. 1 (2018) 963–969, https://doi.org/10.1021/acsaem.8b00009.
[42] S. Chen, X. Shu, H. Wang, J. Zhang, Thermally driven phase transition of manganese oxide on carbon cloth for enhancing the performance of flexible all-solid-state zinc-air batteries, J. Mater. Chem. A 7 (2019) 19719–19727, https://doi.org/10.1039/c9ta05719f.
[43] Y. Liu, B. Qiao, N. Jia, S. Shi, X. Chen, Z. An, P. Chen, Efficient bifunctional oxygen electrocatalysts for rechargeable zinc-air battery: $Fe_3O_4$/N−C nanoflowers derived from aromatic polyamide, ChemCatChem. 14 (2022) 4–12, https://doi.org/10.1002/cctc.202101523.
[44] B. Wang, Y. Ye, L. Xu, Y. Quan, W. Wei, W. Zhu, H. Li, J. Xia, Space-confined yolk-shell construction of $Fe_3O_4$ nanoparticles inside N-doped hollow mesoporous carbon spheres as bifunctional electrocatalysts for long-term rechargeable zinc-air batteries, Adv. Funct. Mater. 30 (2020) 1–8, https://doi.org/10.1002/adfm.202005834.